Asian Journal of Control, Vol. 21, No. 3, pp. 1064–1076, May 2019

FEEDBACK LINEARIZATION CONTROL FOR SYSTEMS WITH MISMATCHED UNCERTAINTIES VIA DISTURBANCE OBSERVERS

Erkan Kayacan and Thor I. Fossen

ABSTRACT

This paper focuses on a novel feedback linearization control (FLC) law based on a self-learning disturbance observer (SLDO) to counteract mismatched uncertainties. The FLC based on BNDO (FLC-BNDO) demonstrates robust control performance only against mismatched time-invariant uncertainties while the FLC based on SLDO (FLC-SLDO) demonstrates robust control performance against mismatched time-invariant and -varying uncertainties, and both of them maintain the nominal control performance in the absence of mismatched uncertainties. In the estima-tion scheme for the SLDO, the BNDO is used to provide a conventional estimation law, which is used as the learning error for the type-2 neuro-fuzzy system (T2NFS), and T2NFS learns mismatched uncertainties. Thus, the T2NFS takes the overall control of the estimation signal entirely in a very short time and gives unbiased estimation results for the dis-turbance. A novel learning algorithm established on sliding mode control theory is derived for an interval type-2 fuzzy logic system. The stability of the overall system is proven for a second-order nonlinear system with mismatched uncer-tainties. The simulation results show that the FLC-SLDO demonstrates better control performance than the traditional FLC, FLC with an integral action (FLC-I), and FLC-BNDO.

Key Words: Disturbance observer, feedback linearization control, mismatched uncertainty, uncertain systems.

I. INTRODUCTION

Uncertainties, for examples, unmodelled dynamics, parameter variations, and disturbances, are inevitable in real-time applications [1]. Since control performance is violated by these uncertainties, disturbance attenuation has a major influence on control system design [2–5]. Therefore, control algorithms based on disturbance observers have been developed to counteract uncertainties in systems [6–8]. In this approach, the main idea is to merge all uncertainties into one term and to add the estimated value of the disturbance by a disturbance observer into a control law that is derived for a disturbance-free model. This control structure has been successfully applied in many applications, such as reusable launch vehicles [9], direct drive motors [10], robot manipulators [11,12], ball mill grinding circuits [13], pulse width modulated inverter [14], inverted pendulum [15], nonuniform wind turbine tower [16], uninterruptible power supplies [17], and dynamic positioning system of ships [18]. Moreover, many controllers, such as adaptive fuzzy-neural control [19] and sliding mode control (SMC) [15,20], have been designed based on disturbance observers.

Uncertainties can be broadly categorized into two groups: matched and mismatched uncertainties [21]. Disturbance and control input appear in the same channel in the former case while they appear in different channels in the latter case [22,23]. In control of systems with matched uncertainties, there exist many successful applications. The reason is that, since the control input is in the same channel as the disturbance, only estimated disturbance value is added into the traditional control law. However, traditional control methods based on a disturbance observer fail to drive states of systems with mismatched uncertainties to the desired equilibrium point so that there deriving novel control laws is necessary [24]. The first solution is to add an integral action to control laws to remove steady-state error [25]. This results in robust control performance against mismatched time-invariant uncertainties but may violate the nominal performance in the absence of a mismatch. The other solution is to derive novel control laws. For example, a novel SMC method has been proposed in [20] by

Manuscript received April 15, 2017; revised December 6, 2017; accepted February 4, 2018.

Erkan Kayacan is with the Coordinated Science Lab, University of Illinois at Urbana-Champaign, Urbana, Illinois 61801, USA (corresponding author, e-mail: erkank@illinois.edu).

Thor I. Fossen is with the Department of Engineering Cybernetics, Center for Autonomous Marine Operations and Systems, Norwegian University of Science and Technology, Trondheim, Norway (e-mail: thor.fossen@ntnu.no).

This work was supported by the Norwegian Research Council (Grant No. 223254) through the Center of Autonomous Marine Operations and Systems (NTNU AMOS) at the Norwegian University of Science and Technology. Present address: Erkan Kayacan, Senseable City Laboratory, Computer Science & Artificial Intelligence Laboratory Massachusetts Institute of Technology, MIT 9-250, 77 Massachusetts Avenue, Cambridge, MA 02139 USA.

proposing a new sliding surface for second-order nonlinear systems with mismatched uncertainties. The simulation results show that the proposed control method provides robust control performance against mismatched uncertainties and also maintains the nominal performance in the absence of mismatched uncertainties.

Another novel SMC method for nth order nonlinear systems with mismatched uncertainties can be found in [24]. A memoryless and memory-based integral sliding surfaces and integral sliding-mode controllers for continuous-time linear systems with mismatched uncertainties in [26], a back-stepping control method for nonlinear systems with mismatched uncertainties in [27], and H_∞ controller based on a nonlinear DO in [28] have been developed recently. Moreover, a comprehensive study of disturbance observer-based control methods has been given in [29].

In the disturbance observer based control approach, uncertainties are represented as a parameter in system models, and thus online parameter estimation methods are required. There are nonlinear state and parameter estimation methods, such as particle filtering method and extended Kalman filter [30–33]. However, it has been reported that the former becomes practically unsolvable in real-time for a large number of variables while the latter is not a good candidate in cases of strong non-linearities [34,35]. Neuro-fuzzy structures with SMC theory-based learning algorithms have been employed for control and identification purposes in feedback-error learning (FEL) schemes [36–40]. In these schemes, a conventional controller works in parallel with a neuro-fuzzy controller in which the output of the conventional controller is used as the learning error to train the neuro-fuzzy controller [41]. After a very short time, the neuro-fuzzy controller takes the overall control signal while the conventional controller converges to zero. Moreover, SMC theory-based learning algorithms ensure robustness and faster convergence rates than the traditional learning methods due to computational simplicity. Motivated by these facts, an FEL estimation scheme is proposed in this study due to computational simplicity and learning capability.

The main contributions of this paper, beyond the existing state-of-the-art, are as follows. First, a novel feedback linearization control (FLC) law based on a self-learning DO (SLDO) is developed against mismatched invariant and varying uncertainties, and the stability of the overall system is proven by taking the SLDO dynamics into account. Second, the SLDO is designed in the FEL scheme in which the conventional estimation law and type-2 neuro-fuzzy structure (T2NFS) work in parallel while the former is used as the learning error for the T2NFS. Thus, the FEL algorithm is employed to develop an observer for the first time. Third, novel SMC theory-based learning rules are proposed for the tuning of the T2NFS. In addition to the stability of the training algorithm, the stability of the SLDO is proven with Lyapunov stability analysis. To the best knowledge of the authors, this is also the first-time such a stability analysis has been proven. Fourth, type-2 fuzzy logic systems are examined under noisy conditions, and computationally efficient disturbance observers are developed.

The paper consists of five sections. Problem formulation is outlined in Section II. The novel FLC law based on the SLDO is formulated, and the stability of the overall system is proven in Section III. The simulation results are presented in Section IV. Finally, a brief conclusion is given in Section V.

II. PROBLEM FORMULATION

A second-order nonlinear system with mismatched uncertainties is written in the following form:

$$\begin{aligned} \dot{x}_1 &= x_2 + d \\ \dot{x}_2 &= a(\mathbf{x}) + b(\mathbf{x})u \\ y &= x_1 \end{aligned} \tag{1}$$

where x_1 and x_2 denote the states, u denotes the control input, d denotes the disturbance, y denotes the output, $a(\mathbf{x})$ and $b(\mathbf{x})$ denote the nonlinear system dynamics.

2.1 Traditional FLC

The traditional FLC law is written as follows:

$$u = -b^{-1}(\mathbf{x})\left(a(\mathbf{x}) + k_1 x_1 + k_2 x_2\right) \tag{2}$$

where k_1, k_2 denote the coefficients of the controller and they are positive, that is, $k_1, k_2 > 0$.

If the control law in (2) is applied to the system with mismatched uncertainties in (1), the closed-loop dynamics are obtained as follows:

$$\ddot{x}_1 + k_2\dot{x}_1 + k_1 x_1 = k_2 d + \dot{d} \tag{3}$$

Remark 1. Eq. (3) shows that the state cannot drive the desired equilibrium point under the control law proposed in (2). This implies why the FLC is sensitive to mismatched uncertainties.

2.2 FLC with integral action

An integral action is added to the control law in order to make the system robust against mismatched uncertainties. The FLC with an integral action (FLC-I)

is formulated as follows:

$$u = -b^{-1}(\mathbf{x})\left(a(\mathbf{x}) + k_1 x_1 + k_2 x_2 + k_i \int_0^t x_1\, dt\right) \tag{4}$$

where k_i denotes the coefficient for the integral action and is positive, that is, $k_i > 0$.

If the control law in (4) is applied to the system with mismatched uncertainties in (1), the closed-loop dynamics are obtained as follows:

$$\dddot{x}_1 + k_2\ddot{x}_1 + k_1\dot{x}_1 + k_i\dot{x}_1 = k_2\dot{d} + \ddot{d} \tag{5}$$

This implies that if the disturbance has a steady-state value, that is, $\dot{d} = \ddot{d} = 0$, the state can be driven to the desired equilibrium point.

Remark 2. Eq. (5) shows that if disturbance has a steady-state value, that is, $\dot{d} = \ddot{d} = 0$, the FLC-I is robust to mismatched time-invariant uncertainties and thus the steady-state error is eliminated. However, adding an integral action can result in a worse performance than the nominal performance obtained by the FLC in the absence of mismatched uncertainties.

2.3 FLC for mismatched time-invariant uncertainties

2.3.1 Basic nonlinear disturbance observer

The second-order nonlinear system with mismatched uncertainties in (1) can be rewritten in the following form:

$$\begin{aligned} \dot{\mathbf{x}} &= \mathbf{g}_1(\mathbf{x}) + \mathbf{g}_2(\mathbf{x})u + \mathbf{z}d \\ y &= x_1 \end{aligned} \tag{6}$$

where $\mathbf{x} = [x_1, x_2]^T$ denotes the state vector, u denotes the control input, d denotes the disturbance, y denotes the output, $\mathbf{g}_1(\mathbf{x}) = [x_2, a(\mathbf{x})]^T$ and $\mathbf{g}_2(\mathbf{x}) = [0, b(\mathbf{x})]^T$ denote the nonlinear system dynamics, and $\mathbf{z} = [1, 0]^T$ denotes the disturbance coefficient vector.

The BNDO has been proposed in [42–44] for uncertainty problem to estimate the disturbance as follows:

$$\begin{aligned} \dot{p} &= -\mathbf{l}\mathbf{z}p - \mathbf{l}\left(\mathbf{z}\mathbf{l}\mathbf{x} + \mathbf{g}_1(\mathbf{x}) + \mathbf{g}_2(\mathbf{x})u\right) \\ \hat{d}_{BN} &= p + \mathbf{l}\mathbf{x} \end{aligned} \tag{7}$$

where $\hat{d}_{BN}$ denotes the disturbance estimation, p and $\mathbf{l} = [\,l_1,\ l_2\,]$ denote the internal state and observer gain vector of the BNDO, respectively.

The time-derivative of the disturbance estimation is derived from (7) as follows:

$$\dot{\hat{d}}_{BN} = \mathbf{l}\mathbf{z}\, e_d \tag{8}$$

where $e_d = d - \hat{d}_{BN}$ denotes the estimation error for the disturbance. Since $\mathbf{z} = [\,1\ 0\,]^T$ in (1), it is obtained as follows:

$$\dot{\hat{d}}_{BN} = l_1 e_d \tag{9}$$

The error dynamics of the BNDO are obtained by adding the disturbance rate $\dot{d}$ into (8) as:

$$\dot{e}_d + l_1 e_d = \dot{d} \tag{10}$$

Assumption 1. The time-derivative of the disturbance is bounded and has a steady-state value, that is, $\lim_{t\to\infty} \dot{d}(t) = 0$.

If Assumption 1 is satisfied, then (10) is obtained as follows:

$$\dot{e}_d + l_1 e_d = 0 \tag{11}$$

Lemma 1. [42]. If l_1 is positive, i.e., $l_1 > 0$, the error dynamics of the BNDO in (11) converge to zero exponentially.

Lemma 1 implies that the estimated disturbance by the BNDO can track the actual disturbance of the system in (1) exponentially if the disturbance has a steady-state value.

2.3.2 Controller design

A novel FLC law based on the BNDO to handle mismatched time-invariant uncertainties as shown in Fig. 1 is formulated as follows:

$$u = -b^{-1}(\mathbf{x})\left(a(\mathbf{x}) + k_1 x_1 + k_2(x_2 + \hat{d}_{BN})\right) \tag{12}$$

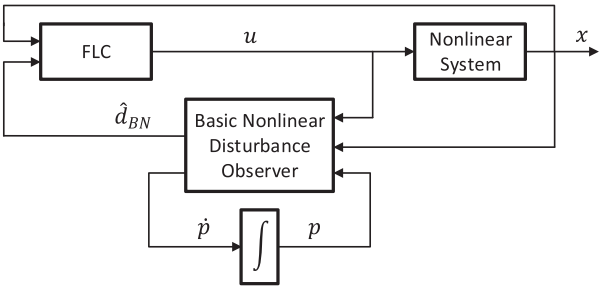

Fig. 1. The diagram of the disturbance observer (DO).

If the aforementioned control law in (12) is applied to the second-order nonlinear system in (1), the closed-loop dynamics are obtained as

$$\ddot{x}_1 + k_2\dot{x}_1 + k_1 x_1 = k_2 e_d + \dot{d} \tag{13}$$

If Assumption 1 is satisfied, the closed-loop dynamics are obtained as follows:

$$\ddot{x}_1 + k_2\dot{x}_1 + k_1 x_1 = k_2 e_d \tag{14}$$

Lemma 2. [45]. If a nonlinear system $\dot{\mathbf{x}} = F(\mathbf{x}, \mathbf{u})$ is input-state stable and $\lim_{t\to\infty} \mathbf{u}(t) = 0$, then the state $\lim_{t\to\infty} \mathbf{x}(t) = 0$.

The closed-loop dynamics in (14) are stable if the coefficients are positive, that is, $k_1, k_2 > 0$. As indicated in Lemma 2, if the input satisfies $\lim_{t\to\infty} e_d(t) = 0$, then the state satisfies $\lim_{t\to\infty} x_1(t) = 0$.

The closed-loop error dynamics in (11) and (14) are combined as follows:

$$\begin{aligned} \dot{e}_d + l_1 e_d &= 0 \\ \ddot{x}_1 + k_2\dot{x}_1 + k_1 x_1 &= k_2 e_d \end{aligned} \tag{15}$$

The closed-loop error dynamics are globally exponentially stable under the given condition $k_1, k_2, l_1 > 0$ and the states satisfy $\lim_{t\to\infty} x_1(t) = 0$ and $\lim_{t\to\infty} e_d(t) = 0$. This implies that the states can be driven to the desired equilibrium point.

Remark 3. The FLC based on the BNDO (FLC-BNDO) is robust to mismatched time-invariant uncertainties. If there exists no disturbance, the FLC-BNDO maintains the nominal control performance as distinct from the FLC-I.

Remark 4. If the time-derivative of the disturbance $\dot{d}$ is time-varying, the error dynamics of the BNDO cannot converge to zero. Therefore, there exists always a difference between the estimated and true values of the disturbance so that the FLC-BNDO cannot be robust to mismatched time-varying uncertainties.

III. NEW FLC FOR MISMATCHED TIME-VARYING UNCERTAINTIES

3.1 Self-learning disturbance observer

An SLDO is developed in this section due to the fact that the BNDO (7) cannot estimate time-varying disturbances as stated in Remark 4. In this investigation, a feedback-error learning (FEL) scheme in which the conventional estimation law works in parallel with a T2NFS is proposed as the diagram of the SLDO is illustrated in Fig. 2. The new estimation law is proposed as follows:

$$\tau = \tau_c - \tau_n \tag{16}$$

where τ_c and τ_n denote respectively the outputs of the conventional estimation law and T2NFS. A conventional proportional-derivative estimation law in the FEL scheme is used to guarantee the global asymptotic stability of the SLDO in a compact space. The input to FEL algorithm is the output of the BNDO and the time-derivative of its output $\dot{\hat{d}}_{BN}$ is equal to the multiplication of the disturbance estimation error and the observer gain of the BNDO as can be seen from (9). Therefore, the conventional estimation law is formulated as follows:

$$\tau_c = \dot{\hat{d}}_{BN} + \eta\ddot{\hat{d}}_{BN} \tag{17}$$

where η is the coefficient and positive, that is, $\eta > 0$, and d_{BN} is the output of the BNDO.

3.1.1 Type-2 neuro-fuzzy structure

An interval type-2 Takagi-Sugeno-Kang fuzzy *if-then* rule R_{ij} is written as:

$$R_{ij}: \text{ If } \xi_1 \text{ is } \tilde{1}_i \text{ and } \xi_2 \text{ is } \tilde{2}_j, \text{ then } f_{ij} = \Upsilon_{ij} \tag{18}$$

where $\xi_1 = \dot{\hat{d}}_{BN}$ and $\xi_2 = \ddot{\hat{d}}_{BN}$ denote the inputs while $\tilde{1}_i$ and $\tilde{2}_j$ denote type-2 fuzzy sets for inputs. The function f_{ij} is the output of the rules and the total number of the rules are equal to $K = I \times J$ in which I and J are the total number of the inputs.

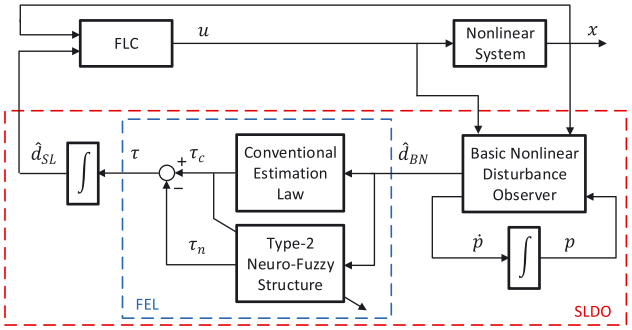

Fig. 2. The diagram of the self-learning disturbance observer (SLDO). [Color figure can be viewed at wileyonlinelibrary.com]

The upper and lower Gaussian membership functions for type-2 fuzzy logic systems are written as follows:

$$\underline{\mu}_{1i}(\xi_1) = \exp\left(-\left(\frac{\xi_1 - \underline{c}_{1i}}{\underline{\sigma}_{1i}}\right)^2\right) \tag{19}$$

$$\overline{\mu}_{1i}(\xi_1) = \exp\left(-\left(\frac{\xi_1 - \overline{c}_{1i}}{\overline{\sigma}_{1i}}\right)^2\right) \tag{20}$$

$$\underline{\mu}_{2j}(\xi_2) = \exp\left(-\left(\frac{\xi_2 - \underline{c}_{2j}}{\underline{\sigma}_{2j}}\right)^2\right) \tag{21}$$

$$\overline{\mu}_{2j}(\xi_2) = \exp\left(-\left(\frac{\xi_2 - \overline{c}_{2j}}{\overline{\sigma}_{2j}}\right)^2\right) \tag{22}$$

where $\underline{c}, \overline{c}, \underline{\sigma}, \overline{\sigma}$ denote respectively the lower and upper mean, and the lower and upper standard deviation of the membership functions. These parameters are adjustable for the T2NFS in which the standard deviations are positive, that is, $\underline{\sigma}, \overline{\sigma} > 0$.

The lower and upper membership functions $\underline{\mu}$ and $\overline{\mu}$ are determined for every signal. Then, the firing strength of rules are calculated as follows:

$$\underline{w}_{ij} = \underline{\mu}_{1i}(\xi_1)\underline{\mu}_{2j}(\xi_2), \quad \overline{w}_{ij} = \overline{\mu}_{1i}(\xi_1)\overline{\mu}_{2j}(\xi_2) \tag{23}$$

The output of the every fuzzy rule is a linear function f_{ij} formulated in (18). The output of the network is formulated below:

$$\tau_n = q\sum_{i=1}^{I}\sum_{j=1}^{J} f_{ij}\widetilde{\underline{w}}_{ij} + (1-q)\sum_{i=1}^{I}\sum_{j=1}^{J} f_{ij}\widetilde{\overline{w}}_{ij} \tag{24}$$

where $\widetilde{\underline{w}}_{ij}$ and $\widetilde{\overline{w}}_{ij}$ are the normalized firing strengths of the lower and upper output signals of the neuron ij are written as follows:

$$\widetilde{\underline{w}}_{ij} = \frac{\underline{w}_{ij}}{\sum_{i=1}^{I}\sum_{j=1}^{J}\underline{w}_{ij}}, \quad \widetilde{\overline{w}}_{ij} = \frac{\overline{w}_{ij}}{\sum_{i=1}^{I}\sum_{j=1}^{J}\overline{w}_{ij}} \tag{25}$$

The design parameter q weights the participation of the lower and upper firing levels and is generally set to 0.5. In this paper, it is formulated as a time-varying parameter in the next subsection.

The vectors are defined as::

$$\widetilde{\underline{\mathbf{W}}} = [\widetilde{\underline{w}}_{11}\ \widetilde{\underline{w}}_{12} \cdots \widetilde{\underline{w}}_{21} \cdots \widetilde{\underline{w}}_{ij} \cdots \widetilde{\underline{w}}_{IJ}]^T$$
$$\widetilde{\overline{\mathbf{W}}} = [\widetilde{\overline{w}}_{11}\ \widetilde{\overline{w}}_{12} \cdots \widetilde{\overline{w}}_{21} \cdots \widetilde{\overline{w}}_{ij} \cdots \widetilde{\overline{w}}_{IJ}]^T$$
$$\mathbf{F} = [f_{11}\, f_{12} \cdots f_{21} \cdots f_{ij} \cdots f_{IJ}]$$

where these normalized firing strengths are between 0 and 1, that is, $0 < \widetilde{\underline{w}}_{ij} \leq 1$ and $0 < \widetilde{\overline{w}}_{ij} \leq 1$. In addition, $\sum_{i=1}^{I}\sum_{j=1}^{J}\widetilde{\underline{w}}_{ij} = 1$ and $\sum_{i=1}^{I}\sum_{j=1}^{J}\widetilde{\overline{w}}_{ij} = 1$.

3.1.2 SMC theory-based learning algorithm

In the FEL algorithm, the output of the conventional estimation law τ_c must converge to zero while T2NFS is learning; therefore, the proposed sliding surface s for the learning algorithm contains the conventional estimation law and is formulated as follows:

$$s = \tau_c + \frac{\ddot{\hat{d}}_{BN}}{l_1} \tag{26}$$

where s is used as the learning error to train the learning algorithm.

Novel adaptation rules for the T2NFS parameters are proposed in this investigation by the following equations:

$$\dot{\underline{c}}_{1i} = \dot{\overline{c}}_{1i} = \dot{\xi}_1 + \xi_1\alpha\ \mathrm{sgn}(s) \tag{27}$$

$$\dot{\underline{c}}_{2j} = \dot{\overline{c}}_{2j} = \dot{\xi}_2 + \xi_2\alpha\ \mathrm{sgn}(s) \tag{28}$$

$$\dot{\underline{\sigma}}_{1i} = -\frac{\underline{\sigma}_{1i}}{\xi_1 - \underline{c}_{1i}}\left(\xi_1 + \frac{(\underline{\sigma}_{1i})^2}{\xi_1 - \underline{c}_{1i}}\right)\alpha\ \mathrm{sgn}(s) \tag{29}$$

$$\dot{\overline{\sigma}}_{1i} = -\frac{\overline{\sigma}_{1i}}{\xi_1 - \overline{c}_{1i}}\left(\xi_1 + \frac{(\overline{\sigma}_{1i})^2}{\xi_1 - \overline{c}_{1i}}\right)\alpha\ \mathrm{sgn}(s) \tag{30}$$

$$\dot{\underline{\sigma}}_{2j} = -\frac{\underline{\sigma}_{2j}}{\xi_2 - \underline{c}_{2j}}\left(\xi_2 + \frac{(\underline{\sigma}_{2j})^2}{\xi_2 - \underline{c}_{2j}}\right)\alpha\ \mathrm{sgn}(s) \tag{31}$$

$$\dot{\overline{\sigma}}_{2j} = -\frac{\overline{\sigma}_{2j}}{\xi_2 - \overline{c}_{2j}}\left(\xi_2 + \frac{(\overline{\sigma}_{2j})^2}{\xi_2 - \overline{c}_{2j}}\right)\alpha\ \mathrm{sgn}(s) \tag{32}$$

$$\dot{f}_{ij} = -\frac{q\widetilde{\underline{w}}_{ij} + (1-q)\widetilde{\overline{w}}_{ij}}{(q\widetilde{\underline{\mathbf{W}}} + (1-q)\widetilde{\overline{\mathbf{W}}})^T\ (q\widetilde{\underline{\mathbf{W}}} + (1-q)\widetilde{\overline{\mathbf{W}}})}\alpha sgn(s) \tag{33}$$

$$\dot{q} = -\frac{1}{\mathbf{F}(\underline{\widetilde{\mathbf{W}}} - \widetilde{\overline{\mathbf{W}}})^T}\alpha sgn(s) \tag{34}$$

where α is the learning rate and positive, that is, $\alpha > 0$.

Theorem 1 (Stability of the learning algorithm)**.** If adaptations rules are proposed as in (27)-(34) and the learning rate α is large enough, i.e., $\alpha > \dot{\tau}^* \frac{|\tau_c + \dot{e}_d| + |\dot{e}_d|}{|\tau_c + \dot{e}_d| - |\dot{e}_d|}$ where $\dot{\tau}^*$ is the upper bound of $\dot{\tau}$, this ensures that τ_c will converge to zero in finite time for a given arbitrary initial condition $\tau_c(0)$.

Proof 1. The Lyapunov function is written as follows:

$$V = \frac{1}{2}\tau_c^2 \tag{35}$$

By taking the time-derivative of the Lyapunov function in (35), it is obtained as

$$\dot{V} = \tau_c \dot{\tau}_c \tag{36}$$

If the time-derivative of the conventional estimation law $\dot{\tau}_c$ is derived from (16) and then is inserted into the equation above:

$$\dot{V} = \tau_c(\dot{\tau}_n + \dot{\tau}) \tag{37}$$

The calculation of $\dot{\tau}_n$ in (70) is inserted into (37), it is obtained as follows:

$$\dot{V} = \tau_c\left(-2\alpha \text{sgn}\,(s) + \dot{\tau}\right) \tag{38}$$

The sliding surface in (26) is inserted into the aforementioned equation

$$\dot{V} = \tau_c\left(-2\alpha \text{sgn}\left(\tau_c + \frac{\ddot{\hat{d}}_{BN}}{l_1}\right) + \dot{\tau}\right) \tag{39}$$

It is obtained considering (9) as follows:

$$\begin{aligned}\dot{V} &= \tau_c\left(-2\alpha\ \text{sgn}\left(\tau_c + \dot{e}_d\right) + \dot{\tau}\right) \\ &= \left(\tau_c + \dot{e}_d\right)\left(-2\alpha\ \text{sgn}\left(\tau_c + \dot{e}_d\right) + \dot{\tau}\right) \\ &\quad - \dot{e}_d\left(-2\alpha\ \text{sgn}\left(\tau_c + \dot{e}_d\right) + \dot{\tau}\right)\end{aligned} \tag{40}$$

If it is assumed that $\dot{\tau}$ is upper bounded by $\dot{\tau}^*$, (40) is obtained as follows:

$$\begin{aligned}\dot{V} &< |\ \tau_c + \dot{e}_d\ |\,(-2\alpha + \dot{\tau}^*) + |\ \dot{e}_d\ |\,(2\alpha + \dot{\tau}^*) \\ &< -2\alpha\left(|\ \tau_c + \dot{e}_d\ | - |\ \dot{e}_d\ |\right) \\ &\quad + \dot{\tau}^*\left(|\ \tau_c + \dot{e}_d\ | + |\ \dot{e}_d\ |\right) \\ &< -2\alpha + \dot{\tau}^* \frac{|\ \tau_c + \dot{e}_d\ | + |\ \dot{e}_d\ |}{|\ \tau_c + \dot{e}_d\ | - |\ \dot{e}_d\ |}\end{aligned} \tag{41}$$

As stated in Theorem 1, if the learning rate α is large enough, that is, $\alpha > \dot{\tau}^* \frac{|\tau_c + \dot{e}_d| + |\dot{e}_d|}{|\tau_c + \dot{e}_d| - |\dot{e}_d|}$, then the time-derivative of the Lyapunov function is negative, that is, $\dot{V} < 0$, so that the SMC theory-based learning algorithm is globally asymptotically stable and τ_c will converge to zero in finite time.

3.1.3 Stability of SLDO

The proposed SLDO law in (16) is re-written taking (17) into account as follows:

$$\tau = \dot{\hat{d}}_{BN} + \eta\ddot{\hat{d}}_{BN} - \tau_n \tag{42}$$

The error dynamics for the SLDO are obtained by adding the actual disturbance rate $\dot{d}$ into the estimated disturbance rate in (42) and considering the dynamics of the time-derivative of the estimated disturbance by BNDO in (8) and $\tau = \dot{\hat{d}}_{SL}$:

$$\begin{aligned}\dot{d} - \dot{\hat{d}}_{SL} &= -\dot{\hat{d}}_{BN} - \eta\ddot{\hat{d}}_{BN} + \tau_n + \dot{d} \\ \dot{e}_d &= -l_1 e_d - \eta l_1 \dot{e}_d + \tau_n + \dot{d}\end{aligned} \tag{43}$$

By taking the time-derivative of (43), it is obtained as follows:

$$\ddot{e}_d = \frac{-l_1\dot{e}_d + \dot{\tau}_n + \ddot{d}}{1 + \eta l_1} \tag{44}$$

As calculated in Appendix, $\dot{\tau}_n = -2\alpha sgn(s)$ is inserted into (44);

$$\ddot{e}_d = \frac{-l_1\dot{e}_d - 2\alpha sgn(s) + \ddot{d}}{1 + \eta l_1} \tag{45}$$

If τ_c in (17) is inserted into (26), the sliding surface is obtained as follows:

$$s\left(\dot{\hat{d}}_{BN}, \ddot{\hat{d}}_{BN}\right) = (\eta + \frac{1}{l_1})\ddot{\hat{d}}_{BN} + \dot{\hat{d}}_{BN} \tag{46}$$

Theorem 2 (Stabiltiy of the SLDO)**.** The estimation law in (16) is employed as a DO, the closed-loop error dynamics for the SLDO are asymptotically stable if the learning rate of the T2NFS α is large enough, that is, $\alpha > \ddot{d}^*$ where the acceleration of the actual disturbance $\ddot{d}$ is upper bounded by $\ddot{d}^*$.

Proof 2. The Lyapunov function is written as follows:

$$V = \frac{1}{2}s^2 \tag{47}$$

By taking the time-derivative of the Lyapunov function above, it is obtained as

$$\dot{V} = s\dot{s} \tag{48}$$

If the time-derivative of the sliding surface in (46) is inserted into the aforementioned equation, it is obtained as follows:

$$\dot{V} = s\left(\dddot{\hat{d}}_{BN}(\eta + \frac{1}{l_1}) + \ddot{\hat{d}}_{BN}\right) \tag{49}$$

The aforementioned equation is obtained considering (9)

$$\dot{V} = s\left(\ddot{e}_d(\eta l_1 + 1) + l_1\dot{e}_d\right) \tag{50}$$

(45) is inserted into (50), it is obtained as follows:

$$\dot{V} = s\left((\frac{-l_1\dot{e}_d - 2\alpha sgn(s) + \ddot{d}}{1 + \eta l_1})(\eta l_1 + 1) + l_1\dot{e}_d\right) \tag{51}$$

If it is assumed that $\ddot{d}$ is upper bounded by $\ddot{d}^*$:

$$\dot{V} < \mid s \mid (-2\alpha + \ddot{d}^*) \tag{52}$$

As stated in Theorem 2, if the learning rate α is large enough, i.e., $\alpha > \ddot{d}^*$, then the time-derivative of the Lyapunov function is negative, that is, $\dot{V} < 0$, so that the SLDO is globally asymptotically stable. This purports that the closed-loop error dynamics for the SLDO converge to zero.

3.2 Controller design

A novel control law based on the SLDO by taking the estimated values of the disturbance and disturbance rate into account are given as follows:

$$u = -b^{-1}(\mathbf{x})\left(a(\mathbf{x}) + k_1x_1 + k_2(x_2 + \hat{d}_{SL}) + \dot{\hat{d}}_{SL}\right) \tag{53}$$

If the aforementioned control law in (53) is applied to the second-order nonlinear system in (1), the closed-loop dynamics are obtained as

$$\ddot{x}_1 + k_2\dot{x}_1 + k_1x_1 = k_2e_d + \dot{e}_d \tag{54}$$

where e_d and $\dot{e}_d$ denote the estimation errors for the disturbance and disturbance rate, respetively.

As stated in Theorem 2, e_d can converge to zero and the closed-loop error dynamics (54) is stable if the coefficients are positive, that is, $k_1, k_2 > 0$. Therefore, since the input satisfies $\lim_{t\to\infty} e_d(t) = 0$ and the state satisfies $\lim_{t\to\infty} x_1(t) = 0$ as stated in Lemma 2. This implies that the states can be driven to the desired equilibrium point asymptotically under the control law in (53) based on the SLDO.

Remark 5. The FLC based on the SLDO (FLC-SLDO) is robust to mismatched time-varying uncertainties and maintains the nominal control performance in case of no disturbance.

IV. SIMULATION STUDIES

The controllers designed in this paper are applied to a second-order nonlinear system, which is formulated as follows

$$\begin{aligned}\dot{x}_1 &= x_2 + d\\ \dot{x}_2 &= -x_1 - x_2 + 0.3\cos(x_1) + e^{x_1} + u\end{aligned} \tag{55}$$

where $a(x) = -x_1 - x_2 + 0.3\cos(x_1) + e^{x_1}$, $b(x) = 1$ and $z = [1, 0]^T$ as can be seen from (1).

SMC theory suffers from high-frequency oscillations called *chattering* because of the discontinuous term. Several approaches have been suggested to avoid chattering. One of the popular ways is to replace the sign function by an approximate $sgn(s) = s/(|s| + \delta)$, which mimics a high gain control [46]. In this paper, the *sgn* functions are replaced by the following equation to decrease the chattering effect:

$$\text{sgn}\,(s) := \frac{s}{\mid s \mid + 0.05} \tag{56}$$

The initial conditions on the states are set to $\mathbf{x}(0) = [1, 1]^T$. The coefficients of the FLCs are respectively set to $k_1 = 3, k_2 = 5$ and $k_i = 3$. The observer gain of the DO is set to $\mathbf{l} = [l_1, l_2] = [5, 0]$, the coefficient η in (17) is set to $\eta = 10$ and the learning rate α of the SLDO is set to 0.03. The initial condition on the parameter q is set to 0.5. In order to evaluate different controllers in the absence and presence of the mismatched uncertainties, there exists no disturbance imposed on the system at $t = 0 - 20$ second, a step external disturbance $d = 0.5$ is imposed on the system at $t = 20 - 40$ second and a multi-sinusoidal external disturbance $d = 0.25 + 0.15 \times (\sin(0.5t) + \sin(1.5t))$ is imposed on the system at $t = 40 - 60$ second. The sampling time for all the simulations in this study is set to 0.001 second while the number of membership functions are selected as $I = J = 3$.

The responses of the states x_1, x_2 are respectively shown in Figs 3(a)-3(b). In the absence of mismatched uncertainties, all FLCs ensure nominal control performance while FLC-I cannot give nominal control performance due to the integral action as stated in Remark 2. The integral action causes large overshoot,

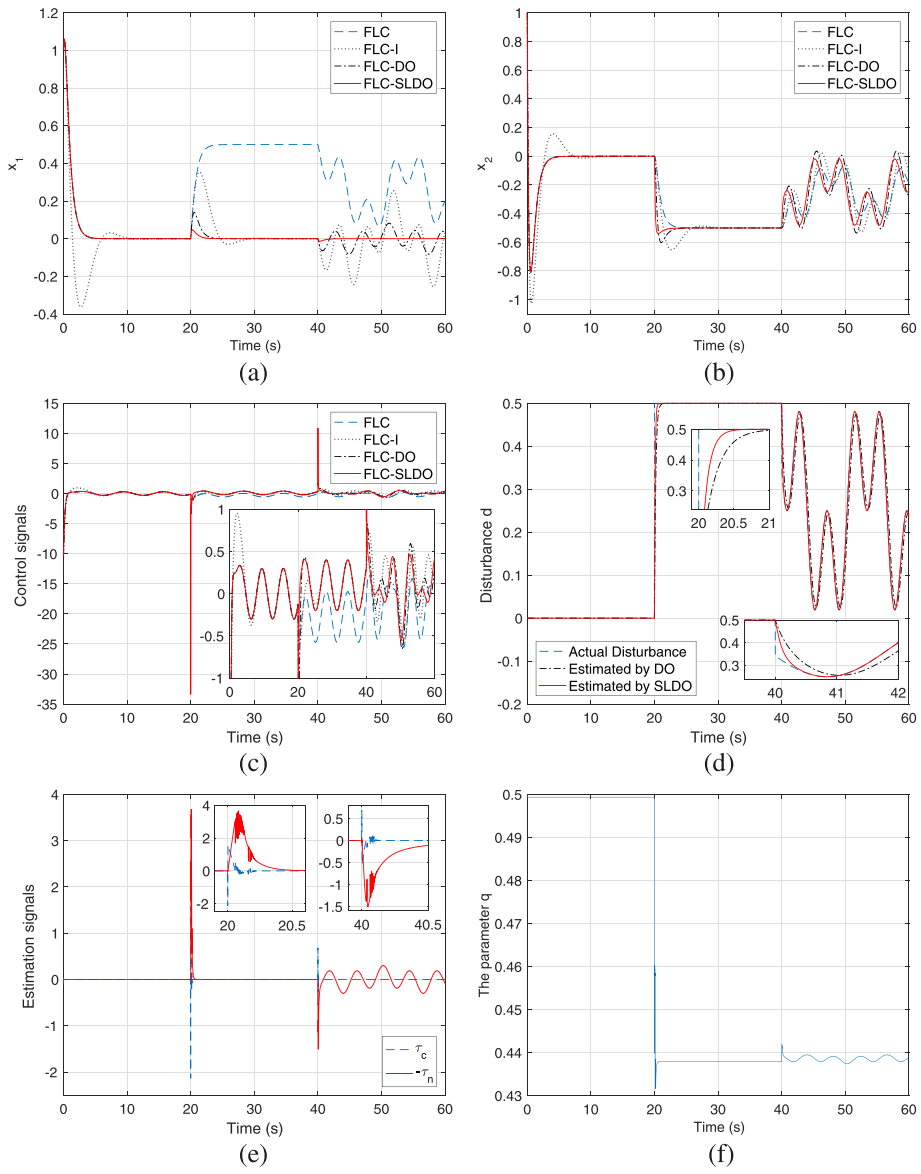

Fig. 3. (a) The responses of state x_1 (b) The responses of state x_2 (c) The control signals (d) The true and estimated values of the distubance (e) The estimation signals (f) The parameter q. [Color figure can be viewed at wileyonlinelibrary.com]

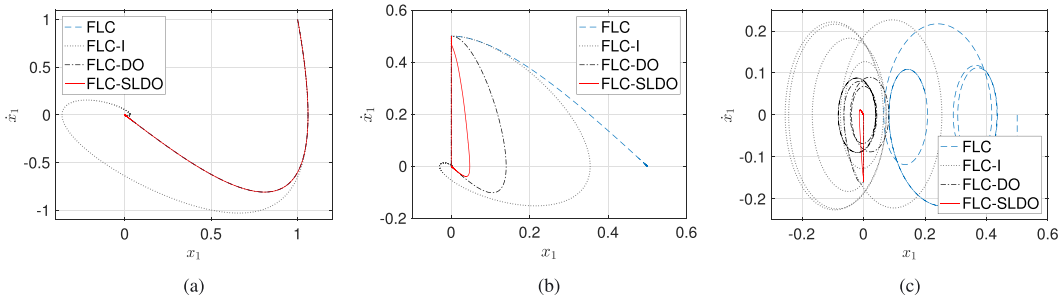

Fig. 4. The phase portraits (a) $t = 0 - 20$ second (b) $t = 20 - 40$ second (c) $t = 40 - 60$ second. [Color figure can be viewed at wileyonlinelibrary.com]

rise time, and settling time. In the presence of mismatched time-invariant uncertainties, the FLC-I, FLC-BNDO, and FLC-SLDO ensure robust control performance while the traditional FLC is sensitive to mismatched uncertainties as stated in Remark 1. Moreover, the FLC-SLDO gives less rise time, settling time, and overshoot than the FLC-I and FLC-BNDO. After $t = 40$ second, a time-varying disturbance is imposed on the system to evaluate controllers against mismatched time-varying uncertainties. As seen, only the FLC-SLDO gives robust control performance while other controllers fail to drive the states to the desired equilibrium point.

The control signals are shown in Fig. 3(c), and the actual and estimated disturbances are shown in Fig. 3(d). The BNDO can estimate only time-invariant disturbances while the SLDO can estimate both time-invariant and time-varying disturbances. Moreover, the SLDO reaches the true disturbance value faster than the BNDO in the presence of time-invariant disturbances. Thanks to learning by the T2NFS, the T2NFS can take the overall control of the estimation signal while the conventional estimation signal τ_c converges to zero in finite time as shown in Fig. 3(e). Thus, the T2NFS becomes the leading estimation signal after a short time-period in the SLDO. The adaptation of the parameter q is shown in Fig. 3(f). Thanks to the adaptation rule in (34), it is adjusted throughout the simulations. Moreover, the phase portraits for all controllers are shown in Figs 4(a)-4(c). The states driven to the desired equilibrium point can be seen.

Type-2 fuzzy membership functions are used in the proposed SLDO structure. It is feasible to downgrade them to type-1 counterparts by equalizing the upper and lower values of parameters in (27)-(32). It is reported that since type-2 fuzzy logic systems have more degrees of freedom than type-1 counterparts, they have the capability of dealing with noisy measurements and uncertainties more adequately [47–49]. For this purpose, in order to compare the performance of T2NFS with its type-1 counterpart under noisy conditions, the outputs of the systems are measured with different noise levels *SNR*. The mean squared errors of disturbance estimation for the different noise levels are given in Table I. As can be seen from this table, the T2NFS gives a smaller error than that of the type-1 neuro-fuzzy structure, and the performance of T2NFS is more remarkable while the noise level is high.

Table I. Mean Squared Error.

	20 (dB)	40 (dB)	80 (dB)
Type-1 NFS	0.6084	0.0133	0.0016
Type-2 NFS	0.5542	0.0129	0.0016
Performance	% 8.90	% 3.76	% 0

V. CONCLUSION AND FUTURE WORK

5.1 Conclusion

In this paper, the FLC-SLDO has been investigated to eliminate mismatched uncertainties on the system and to obtain robust control performance. The simulation results show that FLC-BNDO gives robust control performance against only mismatched time-invariant uncertainties. The stability of the training algorithm of the SLDO and the stability of the FLC-SLDO have been proven, and the simulation results show that FLC-SLDO gives robust control performance against mismatched time-varying uncertainties. Additionally, the FLC-SLDO gives less rise time, settling time, and overshoot than the FLC-BNDO in the presence of mismatched time-invariant uncertainties, and they maintain nominal control performance in the absence of mismatched uncertainties. Thanks to the T2NFS, the T2NFS working in parallel with the conventional estimation law in the FEL scheme can estimate time-varying disturbances as distinct from the BNDO, and cope with uncertainties better than its type-1 counterpart under noisy conditions. The SMC-theory based learning algorithm requires significantly less computation time than the traditional ones, for example, gradient descent and evolutionary training algorithms; therefore, the SLDO is computationally an efficient disturbance observer.

5.2 Future work

The proposed method with its stability analysis is valid for only a second-order nonlinear system with mismatched uncertainties. As a future work, the extension of the SLDO and FLC law for nth order nonlinear systems with mismatched uncertainties are some interesting topics to be investigated.

REFERENCES

1. Kayacan, E., H. Ramon, and W. Saeys, "Robust trajectory tracking error model-based predictive control for unmanned ground vehicles," *IEEE/ASME Trans. Mechatron.*, Vol. 21, No. 2, pp. 806–814 (2016).
2. Lau, J. Y., W. Liang, H. C. Liaw, and K. K. Tan, "Sliding mode disturbance observer-based motion control for a piezoelectric actuator-based surgical device," *Asian J. Control*. https://doi.org/10.1002/asjc.1649.
3. Kayacan, E., E. Kayacan, H. Ramon, and W. Saeys, "Nonlinear modeling and identification of an autonomous tractor-trailer system," *Comput. Electron. Agric.*, Vol. 106, pp. 1–10 (2014).

4. Sun, T., J. Zhang, and Y. Pan, "Active disturbance rejection control of surface vessels using composite error updated extended state observer," *Asian J. Control*, Vol. 19, No. 5, pp. 1802–1811 (2017).
5. Kayacan, E., "Multiobjective h_∞ control for string stability of cooperative adaptive cruise control systems," *IEEE Trans. Intell. Veh.*, Vol. 2, No. 1, pp. 52–61 (2017).
6. Cheng, M.-X. and X.-H. Jiao, "Observer-based adaptive l2 disturbance attenuation control of semi-active suspension with mr damper," *Asian J. Control*, Vol. 19, No. 1, pp. 346–355 (2017).
7. Gao, F., M. Wu, J. She, and W. Cao, "Active disturbance rejection in affine nonlinear systems based on equivalent-input-disturbance approach," *Asian J. Control*, Vol. 19, No. 5, pp. 1767–1776 (2017).
8. Kayacan, E., J. M. Peschel, and G. Chowdhary, "A self-learning disturbance observer for nonlinear systems in feedback-error learning scheme," *Eng. Appl. Artif. Intell.*, Vol. 62, pp. 276–285 (2017).
9. Hall, C. E. and Y. B. Shtessel, "Sliding mode disturbance observer-based control for a reusable launch vehicle," *J. Guid. Control Dyn.*, Vol. 29, No. 6, pp. 1315–1328 (2006).
10. Komada, S., M. Ishida, K. Ohnishi, and T. Hori, "Disturbance observer-based motion control of direct drive motors," *IEEE Trans. Energy Convers.*, Vol. 6, No. 3, pp. 553–559 (1991).
11. Liu, C.-S. and H. Peng, "Disturbance observer based tracking control," *J. Dyn. Syst. Meas. Control*, Vol. 122, No. 2, pp. 332–335 (2000).
12. Oh, Y. and W. K. Chung, "Disturbance-observer-based motion control of redundant manipulators using inertially decoupled dynamics," *IEEE/ASME Trans. Mechatron.*, Vol. 4, No. 2, pp. 133–146 (1999).
13. Chen, X., J. Yang, S. Li, and Q. Li, "Disturbance observer based multi-variable control of ball mill grinding circuits," *J. Process Control*, Vol. 19, No. 7, pp. 1205 –1213 (2009).
14. Yokoyama, T. and A. Kawamura, "Disturbance observer based fully digital controlled pwm inverter for cvcf operation," *IEEE Trans. Power Electron.*, Vol. 9, No. 5, pp. 473–480 (1994).
15. Chen, M. and W.-H. Chen, "Sliding mode control for a class of uncertain nonlinear system based on disturbance observer," *Int. J. Adapt Control Signal Process.*, Vol. 24, No. 1, pp. 51–64 (2010).
16. He, W. and S. S. Ge, "Vibration control of a nonuniform wind turbine tower via disturbance observer," *IEEE/ASME Trans. Mechatron.*, Vol. 20, No. 1, pp. 237–244 (2015).
17. Mattavelli, P., "An improved deadbeat control for ups using disturbance observers," *IEEE Trans. Ind. Electron.*, Vol. 52, No. 1, pp. 206–212 (2005).
18. Du, J., X. Hu, M. Krsti, and Y. Sun, "Robust dynamic positioning of ships with disturbances under input saturation," *Automatica*, Vol. 73, pp. 207 –214 (2016).
19. Leu, Y.-G., T.-T. Lee, and W.-Y. Wang, "Observer-based adaptive fuzzy-neural control for unknown nonlinear dynamical systems," *IEEE Trans. Syst. Man Cybern. Part B Cybern.*, Vol. 29, No. 5, pp. 583–591 (1999).
20. Yang, J., S. Li, and X. Yu, "Sliding-mode control for systems with mismatched uncertainties via a disturbance observer," *IEEE Trans. Ind. Electron.*, Vol. 60, No. 1, pp. 160–169 (2013).
21. Kayacan, E., E. Kayacan, H. Ramon, and W. Saeys, "Towards agrobots: Identification of the yaw dynamics and trajectory tracking of an autonomous tractor," *Comput. Electron. Agric.*, Vol. 115, pp. 78–87 (2015).
22. Ginoya, D., P. Shendge, and S. Phadke, "State and extended disturbance observer for sliding mode control of mismatched uncertain systems," *J. Dyn. Syst. Meas. Control*, Vol. 137, No. 7, pp. 074502 (2015).
23. Yang, J., C. Zhang, S. Li, and X. Niu, "Semi-global exquisite disturbance attenuation control for perturbed uncertain nonlinear systems," *Asian J. Control*, Vol. 19, No. 4, pp. 1608–1619 (2017).
24. Ginoya, D., P. Shendge, and S. Phadke, "Sliding mode control for mismatched uncertain systems using an extended disturbance observer," *IEEE Trans. Ind. Electron.*, Vol. 61, No. 4, pp. 1983–1992 (2014).
25. Chen, C. C., S. S. D. Xu, and Y. W. Liang, "Study of nonlinear integral sliding mode fault-tolerant control," *IEEE/ASME Trans. Mechatron.*, Vol. 21, No. 2, pp. 1160–1168 (2016).
26. Zhang, J., X. Liu, Y. Xia, Z. Zuo, and Y. Wang, "Disturbance observer-based integral sliding-mode control for systems with mismatched disturbances," *IEEE Trans. Ind. Electron.*, Vol. 63, No. 11, pp. 7040–7048 (2016).
27. Sun, H. and L. Guo, "Composite adaptive disturbance observer based control and back-stepping method for nonlinear system with multiple mismatched disturbances," *J. Frankl. Inst.*, Vol. 351, No. 2, pp. 1027–1041 (2014).
28. Wei, X. and L. Guo, "Composite disturbance-observer-based control and h control for complex continuous models," *Int. J. Robust Nonlinear Control*, Vol. 20, No. 1, pp. 106–118 (2010).

29. Chen, W. H., J. Yang, L. Guo, and S. Li, "Disturbance-observer-based control and related methods - an overview," *IEEE Trans. Ind. Electron.*, Vol. 63, No. 2, pp. 1083–1095 (2016).
30. Kayacan, E., E. Kayacan, H. Ramon, and W. Saeys, "Learning in centralized nonlinear model predictive control: Application to an autonomous tractor-trailer system," *IEEE Trans. Control Syst. Technol.*, Vol. 23, No. 1, pp. 197–205 (2015).
31. Kayacan, E., J. M. Peschel, and E. Kayacan, "Centralized, decentralized and distributed nonlinear model predictive control of a tractor-trailer system: A comparative study," *2016 American Control Conference (ACC)*, Boston, MA, pp. 4403–4408 (2016).
32. Kayacan, E., E. Kayacan, H. Ramon, and W. Saeys, "Robust tube-based decentralized nonlinear model predictive control of an autonomous tractor-trailer system," *IEEE/ASME Trans. Mechatron.*, Vol. 20, No. 1, pp. 447–456 (2015).
33. Kayacan, E., E. Kayacan, H. Ramon, and W. Saeys, "Distributed nonlinear model predictive control of an autonomous tractor-trailer system," *Mechatronics*, Vol. 24, No. 8, pp. 926–933 (2014).
34. Haseltine, E. L. and J. B. Rawlings*, "Critical evaluation of extended kalman filtering and moving-horizon estimation," *Ind. Eng. Chem. Res.*, Vol. 44, No. 8, pp. 2451–2460 (2005).
35. Rawlings, J. B. and B. R. Bakshi, "Particle filtering and moving horizon estimation," *Comput. Chem. Eng.*, Vol. 30, No. 1012, pp. 1529 –1541 (2006).
36. Efe, M. . O., O. Kaynak, and X. Yu, "Sliding mode control of a three degrees of freedom anthropoid robot by driving the controller parameters to an equivalent regime," *J. Dyn. Syst. Meas. Control*, Vol. 122, No. 4, pp. 632–640 (2000).
37. Kayacan, E., E. Kayacan, H. Ramon, and W. Saeys, "Adaptive neuro-fuzzy control of a spherical rolling robot using sliding-mode-control-theory-based online learning algorithm," *IEEE T. Cybern.*, Vol. 43, No. 1, pp. 170–179 (2013).
38. Kayacan, E., E. Kayacan, H. Ramon, O. Kaynak, and W. Saeys, "Towards agrobots: Trajectory control of an autonomous tractor using type-2 fuzzy logic controllers," *IEEE/ASME Trans. Mechatron.*, Vol. 20, No. 1, pp. 287–298 (2015).
39. Kayacan, E., W. Saeys, E. Kayacan, H. Ramon, and O. Kaynak, "Intelligent control of a tractor-implement system using type-2 fuzzy neural networks," *2012 IEEE International Conference on Fuzzy Systems*, Brisbane, Queensland, pp. 1–8 (2012).
40. Kayacan, E., E. Kayacan, and M. A. Khanesar, "Identification of nonlinear dynamic systems using type-2 fuzzy neural networks - a novel learning algorithm and a comparative study," *IEEE Trans. Ind. Electron.*, Vol. 62, No. 3, pp. 1716–1724 (2015March).
41. Gomi, H. and M. Kawato, "Neural network control for a closed-loop system using feedback-error-learning," *Neural Netw.*, Vol. 6, No. 7, pp. 933–946 (1993).
42. Chen, W.-H., "Nonlinear disturbance observer-enhanced dynamic inversion control of missiles," *J. Guid. Control Dyn.*, Vol. 26, No. 1, pp. 161–166 (2003).
43. Chen, W.-H., "Disturbance observer based control for nonlinear systems," *IEEE/ASME Trans. Mechatron.*, Vol. 9, No. 4, pp. 706–710 (2004).
44. Yang, J., W. H. Chen, and S. Li, "Non-linear disturbance observer-based robust control for systems with mismatched disturbances/uncertainties," *IET Contr. Theory Appl.*, Vol. 5, No. 18, pp. 2053–2062 (2011).
45. Khalil, H. K. and J. Grizzle, *Nonlinear Systems*, Vol. 3, Prentice hall, New Jersey (1996).
46. Yu, X. and O. Kaynak, "Sliding mode control made smarter: A computational intelligence perspective," *IEEE Syst. Man Cybern. Mag.*, Vol. 3, No. 2, pp. 31–34 (2017).
47. Mendel, J. M., "Uncertainty, fuzzy logic, and signal processing," *Signal Proc.*, Vol. 80, No. 6, pp. 913–933 (2000).
48. Hsiao, M.-Y., T.-H. S. Li, J.-Z. Lee, C.-H. Chao, and S.-H. Tsai, "Design of interval type-2 fuzzy sliding-mode controller," *Inf. Sci.*, Vol. 178, No. 6, pp. 1696–1716 (2008).
49. Khanesar, M., E. Kayacan, M. Teshnehlab, and O. Kaynak, "Analysis of the noise reduction property of type-2 fuzzy logic systems using a novel type-2 membership function," *IEEE Trans. Syst. Man Cybern. Part B Cybern.*, Vol. 41, No. 5, pp. 1395–1406 (2011).

VI. APPENDIX

6.1 Calculation of $\dot{\tau}_n$

By taking the time-derivative of the lower and upper Gaussian membership functions in (19)-(22), the following equations are obtained as:

$$\dot{\underline{\mu}}_{1i}(x_1) = -2\underline{N}_{1i}\dot{\underline{N}}_{1i}\underline{\mu}_{1i}(\xi_1), \tag{57}$$

$$\dot{\overline{\mu}}_{1i}(x_1) = -2\overline{N}_{1i}\dot{\overline{N}}_{1i}\overline{\mu}_{1i}(\xi_1) \tag{58}$$

$$\dot{\underline{\mu}}_{2j}(x_2) = -2\underline{N}_{2j}\dot{\underline{N}}_{2j}\underline{\mu}_{2j}(\xi_2) \tag{59}$$

$$\dot{\overline{\mu}}_{2j}(x_2) = -2\overline{N}_{2j}\dot{\overline{N}}_{2j}\overline{\mu}_{2j}(\xi_2) \tag{60}$$

where

$$\underline{N}_{1i} = \left(\frac{\xi_1 - \underline{c}_{1i}}{\underline{\sigma}_{1i}}\right), \quad \overline{N}_{1i} = \left(\frac{\xi_1 - \overline{c}_{1i}}{\overline{\sigma}_{1i}}\right), \tag{61}$$

$$\underline{N}_{2j} = \left(\frac{\xi_2 - \underline{c}_{2j}}{\underline{\sigma}_{2j}}\right), \quad \overline{N}_{2j} = \left(\frac{\xi_2 - \overline{c}_{2j}}{\overline{\sigma}_{2j}}\right) \tag{62}$$

$$\dot{\underline{N}}_{1i} = \frac{(\dot{\xi}_1 - \dot{\underline{c}}_{1i})\underline{\sigma}_{1i} - (\xi_1 - \underline{c}_{1i})\dot{\underline{\sigma}}_{1i}}{\underline{\sigma}_{1i}^2} \tag{63}$$

$$\dot{\overline{N}}_{1i} = \frac{(\dot{\xi}_1 - \dot{\overline{c}}_{1i})\overline{\sigma}_{1i} - (\xi_1 - \overline{c}_{1i})\dot{\overline{\sigma}}_{1i}}{\overline{\sigma}_{1i}^2} \tag{64}$$

$$\dot{\underline{N}}_{2i} = \frac{(\dot{\xi}_2 - \dot{\underline{c}}_{2i})\underline{\sigma}_{2i} - (\xi_2 - \underline{c}_{2i})\dot{\underline{\sigma}}_{2i}}{\underline{\sigma}_{2i}^2} \tag{65}$$

$$\dot{\overline{N}}_{2i} = \frac{(\dot{\xi}_2 - \dot{\overline{c}}_{2i})\overline{\sigma}_{2i} - (\xi_2 - \overline{c}_{2i})\dot{\overline{\sigma}}_{2i}}{\overline{\sigma}_{2i}^2} \tag{66}$$

By taking the time-derivative of the normalized firing strengths of the lower output signal in (25), the following equation is obtained:

$$\begin{aligned}
\dot{\underline{\widetilde{w}}}_{ij} &= -\underline{\widetilde{w}}_{ij}\underline{K}_{ij} + \underline{\widetilde{w}}_{ij}\sum_{i=1}^{I}\sum_{j=1}^{J}\underline{\widetilde{w}}_{ij}\underline{K}_{ij} \\
\dot{\overline{\widetilde{w}}}_{ij} &= -\overline{\widetilde{w}}_{ij}\overline{K}_{ij} + \overline{\widetilde{w}}_{ij}\sum_{i=1}^{I}\sum_{j=1}^{J}\overline{\widetilde{w}}_{ij}\overline{K}_{ij}
\end{aligned} \tag{67}$$

where

$$\begin{aligned}
\underline{K}_{ij} &= 2\left(\underline{N}_{1i}\dot{\underline{N}}_{1i} + \underline{N}_{2j}\dot{\underline{N}}_{2j}\right) = 4\alpha sgn(s) \\
\overline{K}_{ij} &= 2\left(\overline{N}_{1i}\dot{\overline{N}}_{1i} + \overline{N}_{2j}\dot{\overline{N}}_{2j}\right) = 4\alpha sgn(s)
\end{aligned}$$

The time-derivative of (24) is obtained to find $\dot{\tau}_n$ as follows:

$$\begin{aligned}
\dot{\tau}_n = {} & q\sum_{i=1}^{I}\sum_{j=1}^{J}(\dot{f}_{ij}\underline{\widetilde{w}}_{ij} + f_{ij}\dot{\underline{\widetilde{w}}}_{ij}) \\
& + (1-q)\sum_{i=1}^{I}\sum_{j=1}^{J}(\dot{f}_{ij}\overline{\widetilde{w}}_{ij} + f_{ij}\dot{\overline{\widetilde{w}}}_{ij}) \\
& + \dot{q}\sum_{i=1}^{I}\sum_{j=1}^{J}f_{ij}\underline{\widetilde{w}}_{ij} - \dot{q}\sum_{i=1}^{I}\sum_{j=1}^{J}f_{ij}\overline{\widetilde{w}}_{ij}
\end{aligned} \tag{68}$$

If (67) is inserted to the aforementioned equation:

$$\begin{aligned}
\dot{\tau}_n = {} & q\sum_{i=1}^{I}\sum_{j=1}^{J}\Bigg(\Bigg(-\underline{\widetilde{w}}_{ij}\underline{K}_{ij} + \underline{\widetilde{w}}_{ij}\sum_{i=1}^{I}\sum_{j=1}^{J}\underline{\widetilde{w}}_{ij}\underline{K}_{ij}\Bigg)f_{ij} \\
& + \underline{\widetilde{w}}_{ij}\dot{f}_{ij}\Bigg) + (1-q)\sum_{i=1}^{I}\sum_{j=1}^{J}\Bigg(\Bigg(-\overline{\widetilde{w}}_{ij}\overline{K}_{ij} \\
& + \overline{\widetilde{w}}_{ij}\sum_{i=1}^{I}\sum_{j=1}^{J}\overline{\widetilde{w}}_{ij}\overline{K}_{ij}\Bigg)f_{ij} + \overline{\widetilde{w}}_{ij}\dot{f}_{ij}\Bigg) \\
& + \dot{q}\sum_{i=1}^{I}\sum_{j=1}^{J}f_{ij}(\underline{\widetilde{w}}_{ij} - \overline{\widetilde{w}}_{ij}) \\
= {} & q\sum_{i=1}^{I}\sum_{j=1}^{J}4\alpha sgn(s)\Bigg(\Bigg(-\underline{\widetilde{w}}_{ij} + \underline{\widetilde{w}}_{ij}\sum_{i=1}^{I}\sum_{j=1}^{J}\underline{\widetilde{w}}_{ij}\Bigg)f_{ij} \\
& + \underline{\widetilde{w}}_{ij}\dot{f}_{ij}\Bigg) + (1-q)\sum_{i=1}^{I}\sum_{j=1}^{J}4\alpha sgn(s)\Bigg(\Bigg(-\overline{\widetilde{w}}_{ij} \\
& + \overline{\widetilde{w}}_{ij}\sum_{i=1}^{I}\sum_{j=1}^{J}\overline{\widetilde{w}}_{ij}\Bigg)f_{ij} + \overline{\widetilde{w}}_{ij}\dot{f}_{ij}\Bigg) \\
& + \dot{q}\sum_{i=1}^{I}\sum_{j=1}^{J}f_{ij}(\underline{\widetilde{w}}_{ij} - \overline{\widetilde{w}}_{ij})
\end{aligned} \tag{69}$$

Since $\sum_{i=1}^{I}\sum_{j=1}^{J}\overline{\widetilde{w}}_{ij} = 1$ and $\sum_{i=1}^{I}\sum_{j=1}^{J}\underline{\widetilde{w}}_{ij} = 1$, the aforementioned equation becomes the following by using (33) and (34):

$$\begin{aligned}
\dot{\tau}_n = {} & \sum_{i=1}^{I}\sum_{j=1}^{J}\left(q\underline{\widetilde{w}}_{ij}\dot{f}_{ij} + (1-q)\overline{\widetilde{w}}_{ij}\dot{f}_{ij}\right) \\
& + \dot{q}\sum_{i=1}^{I}\sum_{j=1}^{J}f_{ij}(\underline{\widetilde{w}}_{ij} - \overline{\widetilde{w}}_{ij}) \\
= {} & \left(q\sum_{i=1}^{I}\sum_{j=1}^{J}\underline{\widetilde{w}}_{ij} + (1-q)\sum_{i=1}^{I}\sum_{j=1}^{J}\overline{\widetilde{w}}_{ij}\right)\dot{f}_{ij} \\
& + \dot{q}\sum_{i=1}^{I}\sum_{j=1}^{J}f_{ij}(\underline{\widetilde{w}}_{ij} - \overline{\widetilde{w}}_{ij}) \\
= {} & -2\alpha sgn(s)
\end{aligned} \tag{70}$$